
Dictionary-based Manifold Learning

Hanyu Zhang

Department of Statistics
University of Washington
Seattle, WA 98115
hanyuz6@uw.edu

Samson Koelle

Department of Statistics
University of Washington
Seattle, WA 98115
sjkoelle@gmail.com

Marina Meilă

University of Washington
Seattle, WA 98115
mmp@stat.washington.edu

Abstract

We propose a paradigm for interpretable Manifold Learning for scientific data analysis, whereby we parametrize a manifold with d smooth functions from a scientist-provided *dictionary* of meaningful, domain-related functions. When such a parametrization exists, we provide an algorithm for finding it based on sparse *non-linear* regression in the manifold tangent bundle, bypassing more standard manifold learning algorithms. We also discuss conditions for the existence of such parameterizations in function space and for successful recovery from finite samples. We demonstrate our method with experimental results from a real scientific domain.

1 Introduction

Dimension reduction algorithms map high-dimensional data into a low-dimensional space by a learned function f . However, it is often difficult to ascribe an interpretable meaning to the learned representation. For example, in non-linear methods such as Laplacian Eigenmaps [3] and t-SNE [25], f is learned without construction of an explicit function in terms of the features. In contrast, when scientists describe/model a system using knowledge from their domain, often the resulting model is in terms of domain relevant features, which are continuous functions of other domain variables (e.g. equations of motion).

For example, in the application of Molecule Dynamic Simulation (MDS) study, data are often high dimensional with non-trivial topology, non i.i.d. noise. Figure 1a shows pairwise scatterplots of six toluene molecule features and 1b displays a single scientifically relevant function that model (approximately) the state space of the toluene molecule; it is an angle of rotations.

A functional form f can also be used to compare embeddings from different sources, derive out-of-sample extensions, and to interrogate mechanistic properties of the analyzed system. In figure 1c, we compare the scientifically identified functional mapping f with existing manifold learning algorithms.

This paper proposes to construct a manifold model that interpolates between the two above modalities. Specifically, our algorithm will map samples ξ_i from a manifold to new coordinates $f(\xi_i)$ like in purely data driven manifold learning, but these will be selected from a predefined *finite* set of smooth functions \mathcal{F} , called a *dictionary*, to represent intrinsic manifold coordinates of the data manifold \mathcal{M} . Thus, the obtained embedding is smooth, has closed-form expression, can map new points from the manifold \mathcal{M} to $f(\mathcal{M})$ exactly, and is interpretable with respect to the dictionary.

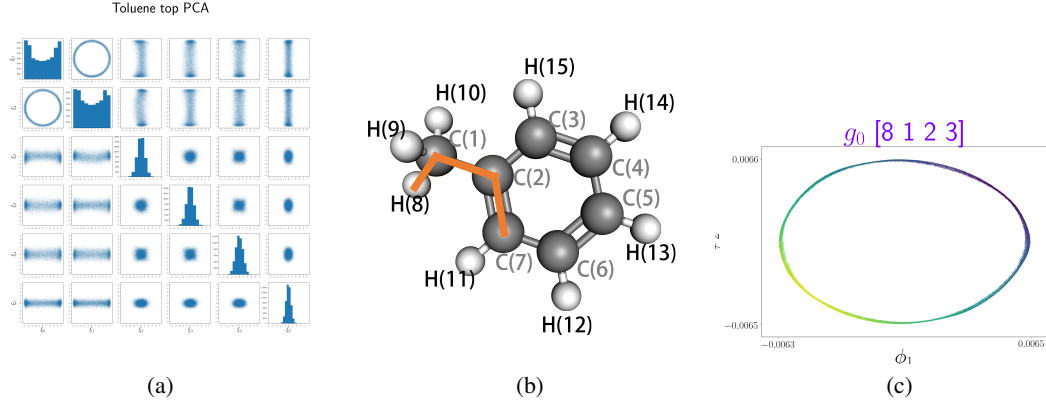


Figure 1: Example of toluene molecule dynamic data. **Left:** pairwise scatterplots of first six coordinates in \mathbb{R}^{50} and histograms of each coordinate on the diagonal. The preprocessing procedure is described in section 5. **Middle:** Atoms in a toluene molecule. Scientists previously discovered that the torsion associated with the peripheral methyl group bound governs the state space of the toluene molecule as a one dimensional manifold. **Right:** Embedding of toluene data into \mathbb{R}^2 by diffusion map, colored by the bond torsion labeled. The variation of the color along the circle demonstrates this function as parametrizing the data manifold.

This method, which we call TSLASSO, requires the key assumption that the manifold \mathcal{M} is parametrized by a subset of functions in the dictionary. However, creating dictionaries of meaningful concepts for a scientific domain and finding those elements that well-describe the data manifold is an everyday task in scientific research. We put the subset-selection task on a formal mathematical basis, and exhibit in Section 5 a scientific domain where the assumptions we make hold, and where our method replaces dictionary-based visual inspection of the data manifold.

Problem Statement Suppose data $\mathcal{D} = \{\xi_i, i \in [n]\}$ are sampled from a d -dimensional connected smooth¹ submanifold \mathcal{M} embedded in the Euclidean space \mathbb{R}^D , where typically $D \gg d$. Assume that the intrinsic dimension d is known. \mathcal{M} has the Riemannian metric induced from \mathbb{R}^D . We are also given a dictionary of functions $\mathcal{F} = \{f_j, j \in [p]\}$. All of the functions f_j are defined in the neighborhood of \mathcal{M} in \mathbb{R}^D and take values in some connected subset of \mathbb{R} . We require that they are smooth on \mathcal{M} (as a subset of \mathbb{R}^D), and have analytically computable gradients in \mathbb{R}^D . Our goal is to select d functions in the dictionary, so that the mapping $f_S = (f_j)_{j \in S \subset \mathcal{F}}$ is a diffeomorphism on an open neighborhood $U \subset \mathcal{M}$ to $f_S(U) \subset \mathbb{R}^{|S|}$ at almost everywhere on \mathcal{M} , f_S is then a *global* mapping with fixed number of functions. The learned mapping f_S will be a *valid parametrization* of \mathcal{M} .

The almost everywhere in the previous definition relaxes the usual definition of smooth embedding. Consider the circle embedded in \mathbb{R}^2 by the map $g : t \mapsto (\cos t, \sin t)$ for $t \in \mathbb{R}$. Consider the function defined for $(x, y) : |x^2 + y^2 - 1| \leq 1/2$, then

$$\Theta : (x, y) \mapsto \begin{cases} \arcsin \frac{y}{\sqrt{x^2 + y^2}} & x \geq 0 \\ \pi - \arcsin \frac{y}{\sqrt{x^2 + y^2}}, & x < 0 \end{cases} \quad (1)$$

is a valid parametrization for \mathcal{M} .

We had made two adjustments to standard differential geometry [16]. First, in differential geometry terminology, $(U \subseteq \mathcal{M}, f_S)$ locally is a coordinate *chart* for \mathcal{M} and f_S^{-1} is called a *parameterization* of U . In this paper, we often refer to f_S as the ‘parameterization’, as f_S, f_S^{-1} are diffeomorphisms and are both representative. We argue that f_S is of more immediate interest, since this map consists of interpretable and analytically computable dictionary functions, and f_S^{-1} , while guaranteed to exist on $f_S(U)$, is defined only implicitly in many scenarios.

¹In this paper, by *smooth* manifold or function we mean of class C^l , $l \geq 1$, to be defined in Section 4.

Second, since a manifold may require multiple charts, we relax the requirement that f_S is locally a diffeomorphism everywhere to *almost everywhere*. In the circle example, since the manifold \mathcal{M} is compact, it is not possible to find a single smooth function that can locally be a diffeomorphism everywhere. This relaxation allows us to find d functions parametrizing a d -dimensional compact manifold in our definition.

Our main technique is to operate over gradient fields on \mathcal{M} , which extends Meila et al. [18]. In Section 2, we introduce some backgrounds on gradient fields on manifolds. In Section 3, we present our algorithm TSLASSO in detail. In Section 4, we provide sufficient conditions for selection consistency. Section 5 shows experimental results on simulations and molecular dynamics datasets. Section 6 discusses related work and interesting features of our approach.

2 Preliminaries: Gradients on Manifolds

The reader is referred to Lee [16] for more backgrounds on differential geometry. In this section, we review gradient fields on manifolds, which play a central role in our algorithm. Consider a d -dimensional manifold \mathcal{M} . At point ξ , its tangent space $\mathcal{T}_\xi \mathcal{M}$ can be viewed as the equivalent class of directions of infinitesimal curves passing ξ . For a smooth function $f : \mathcal{M} \mapsto \mathbb{R}$, its differential $Df : \mathcal{T}_\xi \mathcal{M} \mapsto \mathbb{R}$ is a linear map that generalizes directional derivatives in calculus in Euclidean space, characterizing how the value of f varies along different directions in $\mathcal{T}_\xi \mathcal{M}$. The chain rule also holds for compositions of functions on manifolds.

When \mathcal{M} is Riemannian with metric \mathbf{g} , the gradient is a collection of tangent vectors $X(\xi)$, one at each point ξ , such that for all $\xi \in \mathcal{M}$ and all $v \in \mathcal{T}_\xi \mathcal{M}$

$$\langle X(\xi), v \rangle_{\mathbf{g}} = Df(v)|_{\xi}. \quad (2)$$

For example, under the usual Euclidean metric, a function $f : \mathbb{R}^D \mapsto \mathbb{R}$ has a gradient vector $\nabla f(\xi)$ at each point $\xi \in \mathbb{R}^D$ as defined in ordinary multivariate calculus.

For our problem, \mathcal{M} is a d -dimensional manifold embedded in \mathbb{R}^D with inherited metric. $\mathcal{T}_\xi \mathcal{M}$ can be identified as a d -dimensional linear subspace of $\mathcal{T}_\xi \mathbb{R}^D$, whose basis can be represented by an orthogonal $D \times d$ matrix \mathbf{T}_ξ . Let f be a smooth real-valued function, defined on an open neighborhood of \mathcal{M} . There are two points of views for f when it is restricted on \mathcal{M} : (i) as a function on \mathbb{R}^D and has gradient ∇f as usual. (ii) as a function on \mathcal{M} and one can show that the gradient field $\text{grad } f$ given by the coordinate representation $\text{grad } f := \mathbf{T}_\xi^\top \nabla f$ satisfies (2) [16].

More generally, consider a map $F = (f_1, \dots, f_s) : \mathcal{M} \mapsto \mathbb{R}^s$. The differential $DF = (Df_1, \dots, Df_s)$ is then defined to be a linear mapping from $\mathcal{T}_\xi \mathcal{M} \mapsto \mathcal{T}_\xi \mathbb{R}^s$. Under basis \mathbf{T}_ξ , a coordinate representation of DF is $\mathbf{T}_\xi^\top \nabla F$, where ∇F is a $D \times s$ matrix, constructed by row-wise stacking the gradients $\nabla f_1, \dots, \nabla f_s$.

3 The TSLASSO algorithm

The idea of the TSLASSO algorithm is to express the orthonormal bases $\mathbf{T}_\xi \in \mathbb{R}^{D \times d}$ of the manifold tangent spaces $\mathcal{T}_\xi \mathcal{M}$ as sparse linear combinations of dictionary function gradient vector fields. This simplifies the non-linear problem of selecting a best functional approximation to \mathcal{M} to the linear problem of selecting best local approximations in the tangent bundle. If the subset S with $|S| = d$ gives a valid parametrization, in a neighborhood $U_\xi \subset \mathcal{M}$ of almost all point ξ , f_S is a diffeomorphism, i.e. there is some mapping $g : f_S(U_\xi) \mapsto U_\xi$ such that the identity map $f_S \circ g$ is identity map on $f_S(U_\xi)$ and $g \circ f_S$ is the identity map on U_ξ . Thus, in coordinate representation we can denote a matrix representation of $Df_S(\xi)$ by $\mathbf{X}_{\xi,S} = \mathbf{T}_\xi^\top \nabla f_S(\xi) \in \mathbb{R}^{d \times d}$, and further there is some matrix $\mathbf{B}_{\xi,S} \in \mathbb{R}^{d \times d}$ such that for all $\xi \in \mathcal{M}$

$$\mathbf{I}_d = \mathbf{X}_{\xi,S} \mathbf{B}_{\xi,S} \quad (3)$$

according to the chain rule of function composition on manifolds.

For notation simplicity, we will write $\mathbf{X}_{iS}, \mathbf{B}_{iS}, \mathcal{T}_i \mathcal{M}$ as the corresponding quantities at point ξ_i when we are discussing finite sample. We can select $S = [p]$, and simplify the notation of $\mathbf{X}_{iS}, \mathbf{B}_{iS}$

to $\mathbf{X}_i \in \mathbb{R}^{d \times p}$, $\mathbf{B}_i \in \mathbb{R}^{p \times d}$, but crucially, if we do not have colinear gradients, then we can restrict all but d rows of \mathbf{B}_i to be zeros. We can also select $s = \{j\}$, and define $\mathbf{B}_{\cdot j} \in \mathbb{R}^{nd}$ as the vector formed by concatenating $\mathbf{B}_{i\{j\}}$. Stacking $\mathbf{B}_{\cdot j}$ together forms $\mathbf{B} \in \mathbb{R}^{p \times nd}$.

3.1 Loss Function

We now seek a subset $S \subset [p]$ such that (1) only the corresponding nd vectors $\mathbf{B}_{\cdot j} : j \in S$ have non-zero entries and (2) each submatrix \mathbf{X}_{iS} forms a rank d matrix. The previous observation inspires minimizing Frobenius norm $\|\mathbf{I}_d - \mathbf{X}_i \mathbf{B}_i\|_F$ with joint sparsity constraints over rows of \mathbf{B}_i . This sparsity is also induced jointly over all data points.

$$J_{\lambda_n}(\mathbf{B}) = \frac{1}{2} \sum_{i=1}^n \|\mathbf{I}_d - \mathbf{X}_i \mathbf{B}_i\|_F^2 + \frac{\lambda_n}{\sqrt{dn}} \sum_{j=1}^p \|\mathbf{B}_{\cdot j}\|_2. \quad (4)$$

Note that this optimization problem is a variant of Group Lasso [30] that forces group of coefficients of size dn to be zero simultaneously in the regularization path. The details of the tangent space estimation are deferred to Section 3.2. It can be shown this loss function is invariant to local tangent space rotation.

3.2 Tangent Space Estimation

So far we have solved our problem assuming we have access to the tangent space at each point $\xi \in \mathcal{M}$. However, this is rarely true. In practical use, the first step to realize the previous idea of expressing tangent spaces is to estimate them. *Weighted Local Principal Component Analysis* (WL-PCA) algorithm proposed as Singer and Wu [23], Chen et al. [6], Aamari and Levrard [1] are examples to estimate such basis. These methods are shown to have accurate tangent space estimation when the hyperparameters are selected appropriately.

Intuitively, estimating tangent spaces is estimating local covariances matrices centered at each point ξ_i . We therefore select a neighborhood radius parameter r_N and identify $\mathcal{N}_i = \{i' \in [n], \text{ with } \|\xi_i - \xi_{i'}\|_2 \leq r_N\}$ to be all neighbor points of ξ_i within Euclidean (in \mathbb{R}^D) distance r_N so that we can pass into this algorithm.

When compute local covariance matrices, one may weight different points. These weights of each ξ_j in \mathcal{N}_i can be chosen to be proportional some kernel function $K(x)$ such that for all $j \in \mathcal{N}_i$ the weight is proportional to $K_{ij} = K(\|\xi_i - \xi_j\|/\epsilon_N)$, where ϵ_N is a tuning-parameter proportional to r_N in the sense that kernel-values of pairs of non-neighboring points should be close to zero. Any C^2 positive monotonic decreasing function $K(u)$ with compact support is valid; examples including constant kernel $K(u) = 1_{[0,1]}(u)$, Epanechnikov $K(u) = (1 - u^2)1_{[0,1]}(u)$ and Gaussian $K(u) = \exp(-u^2)1_{[0,1]}(u)$ etc. We specifically choose the Gaussian kernel in our experiments since it provides better tangent space estimation empirically, as it weights more on points that are close to where the tangent space is of interest. Given these weights K_{ij} for ξ_j s, the local weighted mean and weighted covariance at ξ_i can be estimated, and singular value decomposition is used to find the basis.

Let $k_i = |\mathcal{N}_i|$ be the number of neighbors of point ξ_i and $\Xi_i = \{\xi_{i'}, i' \in \mathcal{N}_i\} \in \mathbb{R}^{|\mathcal{N}_i| \times D}$ be the corresponding local position matrices. Also denote a column vector of ones of length k by $\mathbf{1}_k$, and define the Singular Value Decomposition algorithm $\text{SVD}(\mathbf{X}, d)$ of matrix \mathbf{X} as outputting \mathbf{V}, Λ , where Λ and \mathbf{V} are the largest d eigenvalues and their corresponding eigenvectors. Tangent space estimation algorithm is displayed in algorithm TANGENTSPACEBASIS.

3.3 The TSLASSO Algorithm

We now present the full TSLASSO approach. Following the logic in 3, we transform our non-linear manifold parameterization support recovery problem into a collection of sparse linear problems in which we express coordinates of individual tangent spaces as linear combinations of gradients of functions from our dictionary. Tangent spaces at each point are estimated in step 4, enabling utilizing gradients of dictionary functions in $\mathcal{T}_\xi \mathcal{M}$ by projecting the gradient $\nabla f_j(\xi_i) \in \mathbb{R}^D$ on to estimated tangent spaces \mathbf{T}_i . Finally we input these gradients into objective function (4) to solve for the support.

Algorithm 1 TANGENTSPACEBASIS

- 1: **Input:** Local dataset Ξ_i , intrinsic dimension d , kernel parameter ϵ_N
 - 2: Compute local kernel weights $K_{i,\mathcal{N}_i} = (K_{ij})_{j \in \mathcal{N}_i} \in \mathbb{R}^{k_i}$.
 - 3: Compute weighted mean $\xi_i = (K_{i,\mathcal{N}_i}^\top \mathbf{1}_{k_i})^{-1} K_{i,\mathcal{N}_i}^\top \Xi_i$
 - 4: Compute weighted local difference matrix $\mathbf{Z}_i = \text{diag}(K_{i,\mathcal{N}_i}^{\frac{1}{2}})(\Xi_i - \mathbf{1}_{k_i} \bar{\xi}_i)$
 - 5: Compute $\mathbf{T}_i, \Lambda \leftarrow \text{SVD}(\mathbf{Z}_i^\top \mathbf{Z}_i, d)$
 - 6: **Output:** \mathbf{T}_i
-

Algorithm 2 TSLASSO

- 1: **Input:** Dataset \mathcal{D} , dictionary \mathcal{F} , intrinsic dimension d , regularization parameter λ_n , radius parameter r_N , kernel parameter ϵ_N .
 - 2: **for** $i = 1, 2, \dots, n$ (or subset $I \subset [n]$) **do**
 - 3: Compute \mathcal{N}_i and Ξ_i using \mathcal{D}, r_N
 - 4: Compute the orthonormal tangent space basis $\mathbf{T}_i \leftarrow \text{TANGENTSPACEBASIS}(\Xi_i, d, \epsilon_N)$
 - 5: Compute $\nabla f_j(\xi_i)$ for $j \in [p]$.
 - 6: Project onto tangent space
 $\mathbf{X}_i = \mathbf{T}_i^\top [\nabla f_j(\xi)]_{j \in [p]}$
 - 7: **end for**
 - 8: Solve for \mathbf{B} by minimizing $J_{\lambda_n}(\mathbf{B})$ in (4).
 - 9: **Output:** $S = \{j \in [p] : \|\mathbf{B}_{\cdot j}\|_2 > 0\}$
-

3.4 Other considerations

Normalization The rescaling of functions f_j will affect the solution of the Group Lasso objective, since functions with larger gradient norm will tend to have smaller $\|\mathbf{B}_{\cdot j}\|$. This can affect the support S recovered. Therefore, we compute $\gamma_j^2 = \frac{1}{n} \sum_{i=1}^n \|\nabla f_j(\xi_i)\|^2$ and set $f_j \leftarrow f_j / \gamma_j$. This approximates normalization by $\|\nabla f_j\|_{L_2(\mathcal{M})}$. Since $|\nabla f_j(\xi_i)|^2 = |\text{grad } f_j(\xi_i)|^2 + |\nabla f_j^\perp(\xi_i)|^2$, where ∇f_j^\perp denotes the component of ∇f_j orthogonal to \mathcal{M} , normalization prior to projection penalizes functions with large ∇f_j^\perp and favors functions whose gradients are more parallel to the tangent space of \mathcal{M} . Note that, in the high-dimensional setting, we expect random functions to have gradient perpendicular to $\mathcal{T}\mathcal{M}$, and so these will be penalized by our normalization strategy.

Computation Note that we do not need to run TSLASSO on our whole dataset in order to take advantage of all of our data, and can instead run on a subset $I \subset [n]$ such that $|I| = n'$. In particular, the search task in identifying the local datasets Ξ_i is $O(Dnn')$, which is significantly less than the time to construct a full neighbor graph for an embedding. For each i , computing the local mean is $O(k_i D)$, and finding the tangent space is $O(k_i D^2 + k_i^3)$. Gradient computation runtime is $O(D)$, but the constant may be large. Projection is $O(dDp)$. For each Group Lasso iteration, the compute time is $O(n' mpd)$ [18].

Tuning For the real data experiments, we select ϵ_N using the method of Joncas et al. [14], while in simulation, we set it proportional to noise. As explained in the next section, we are theoretically motivated by the definition of parameterization to select a support S that has cardinality equal to d , which is assumed to be given, although dimension estimation as in Levina and Bickel [17] could also be appropriate. For λ , we apply binary search to the regularization path from $\lambda = 0$ to $\lambda_{\max} = \max_j (\sum_{i=1}^n (\|\text{grad}_{\mathcal{T}\mathcal{M}} f_j(\xi_i)\|_2^2)^{1/2}$ to find λ s.t. the cardinality of the selected support is d . In the next section, we introduce support recovery conditions for the success of this approach, and introduce a variation of TSLASSO for when they are violated.

4 Support Recovery Guarantee

In this section, we discuss the behavior of TSLASSO theoretically. First, we discuss the existence and uniqueness of a group of functions $f_S \subset \mathcal{F}$ that can serve as a valid parametrization. When such minimal parametrization exists and is unique, we provide sufficient conditions so that TSLASSO cor-

rectly selects this group with high probability w.r.t. sampling on the manifold and this probability converges to one if sample size tends to infinity.

Assumption 4.1. Throughout this section, we assume the followings to be true.

1. \mathcal{M} is a d -dimensional C^ℓ , $\ell \geq 1$ compact manifold with reach $\tau > 0$ embedded in \mathbb{R}^D with inherited Euclidean metric.
2. Data $\{\xi_i\}_{i=1}^n$ are sampled from some probability measure P on the manifold that has a Radon-Nikodym derivative $\pi(\xi)$ with respect to the Hausdorff measure. There exist two positive constants π_{\min}, π_{\max} such that $0 < \pi_{\min} \leq \pi(\xi) \leq \pi_{\max}$ for all $\xi \in \mathcal{M}$.
3. Dictionary $\mathcal{F} = \{f_j(\xi) : j \in [p]\}$ contains p C^1 functions defined on a neighborhood of \mathcal{M} in \mathbb{R}^D . Further assume that $\delta := \inf_{\xi \in \mathcal{M}} \min_{j \in [p]} \|\nabla f_j(\xi)\| > 0$ and denote $\Gamma := \sup_{\xi \in \mathcal{M}} \max_{j \in [p]} \|\nabla f_j(\xi)\|$.
4. $S \subset [p]$, $|S| = d$ is the only subset such that $\text{rank } f_S = d$ a.e. on \mathcal{M} w.r.t. Hausdorff measure.

Assumption 1 on manifold and 2 on sampling are common in the manifold estimation literature (e.g. Aamari and Levraud [1]). The positive reach in 1 will avoid extreme curvature and bizarre behavior of the manifold, and the assumption 2 on the density enforces the uniformity of sampling. Assumption 3 restricts the smoothness of all dictionary functions and ensures that all dictionary functions do not have critical points on \mathcal{M} as a function on \mathbb{R}^D . One should also notice that $\Gamma < \infty$ by the compactness assumption of \mathcal{M} .

Now we are ready to prove support recovery consistency under suitable conditions. Let $\hat{\mathbf{B}}$ be the solution of problem (4) and $S(\hat{\mathbf{B}})$ be the nonzero rows of $\hat{\mathbf{B}}$. We will show that the probability of $S(\hat{\mathbf{B}}) = S$ converges to 1 as n increases. We start by defining

$$b_S = \inf_{\xi: \text{rank } Df_S(\xi) = d} \min_{j \in S} \|\mathbf{B}_{\xi, \{j\}}\|_2 \quad (5)$$

Larger b_S is an indicator of higher strength of signal. Further consider the matrix $\tilde{\mathbf{X}}_\xi$ whose j -th column is $\mathbf{X}_{\xi, j} / \|\nabla f_j(\xi)\|$. Correspondingly we can define $\tilde{\mathbf{X}}_{\xi, S}$ as the submatrix of $\tilde{\mathbf{X}}$ with columns in S . Let $\mathbf{G}_{\xi, S} = \text{diag}\{\|\nabla f_j(\xi)\|\}_{j \in S}$ and define

$$\mu_S = \sup_{\xi \in \mathcal{M}, j \in S, j' \notin S} |\tilde{\mathbf{X}}_{\xi, j}^\top \tilde{\mathbf{X}}_{\xi, j'}|, \quad (6)$$

$$\nu_S = \sup_{\xi \in \mathcal{M}} \|(\tilde{\mathbf{X}}_{\xi, S}^\top \tilde{\mathbf{X}}_{\xi, S})^{-1} - \mathbf{G}_{\xi, S}^2\|. \quad (7)$$

Here ν_S is finite if $\mu_S < 1/(d-1)$, guaranteed by the Gershgorin circle theorem. The parameter μ_S can be thought of as a renormalized incoherence between the functions in S and those not in S ; ν_S is a internal colinearity parameter, which is small when the columns of $\mathbf{X}_S(\xi)$ are closer to orthogonality and the gradient of functions in S are more parallel to the tangent space. We also define

$$\phi_S = \sup_{\xi \in \mathcal{M}} \max_{j \in S} \|\nabla f_j(\xi)\|_2 \quad (8)$$

which upper bounds the Euclidean gradient of functions in S .

Proposition 4.2. Suppose Assumptions 4.1 hold. In algorithm 2, suppose tangent spaces are estimated by WL-PCA in Section 3.2 using Gaussian kernel and bandwidth parameter choice $\epsilon_N = r_N = C((\log n)/(n-1))^{1/d}$ with large enough constant C , and normalization on dictionary is performed as in Section 3.4. If $(1 + \nu_S/\delta^2)^2 \mu_S \phi_S \Gamma d < 1$ and $\lambda_n(1 + \nu_S/\delta^2)^2 < b_S \sqrt{n}/2$, then there is a constant N depending only on $\mathcal{M}, \pi_{\min}, \pi_{\max}$ such that when $n > N$, it holds that

$$\Pr(S(\hat{\mathbf{B}}) = S) \geq 1 - 4\left(\frac{1}{n}\right)^{\frac{2}{d}} \quad (9)$$

The proof is contained in the supplementary material. The main idea is first to find a sufficient condition so that given correct gradient of each function TSLASSO can find the correct support, assuming correct estimation of the tangent space. Then we consider this condition in the case where

gradient is estimated from data and obtain the guarantee by the fact that tangent spaces can be consistently estimated with larger sample size.

There are some differences to be noted of this recovery result compared with classical recovery guarantees in Group Lasso type problems in e.g. Wainwright [26], Obozinski et al. [19], Elyaderani et al. [10]. First, we cannot adopt directly the usual assumption in Lasso literature that each column of \mathbf{X} has unit norm, considering the normalization in Section 3.2. Also, the asymptotic regime we are considering here is only $n \rightarrow \infty$. Although we are using a Group Lasso type optimization problem, the dimension p is fixed since we only consider the fixed dictionary. There is no other conditions between p and n in our result, as required in many literature. Third, the noise structure is not the same as a general Group Lasso problem since the source of noise is estimation of tangent space. Since we are sampling *on the manifold*, there is no noise level parameter that appears in standard Lasso literature. In a simulation experiment, we also explore the behavior of our method on noisy settings.

5 Experiments

We illustrate the behavior of TSLASSO on both synthetic and real data. Our synthetic data sets include a swiss roll in \mathbb{R}^{49} and a rigid ethanol data in \mathbb{R}^{50} and our real datasets are data molecular dynamics simulation (MDS) for three different molecules (Ethanol, Malonaldehyde and Toluene). Due to space limit we only present result of real datasets here. Results on synthetic datasets are included in the supplementary materials.

For all of the experiments, the data consist of n data points in D dimensions. TSLASSO is applied to a uniformly random subset of size $n' = |T|$ using p dictionary functions, and this process is repeated ω number of times. Note that the entire data set is used for tangent space estimation. In our experiments, the intrinsic dimension d is assumed known, but could be estimated by a method such as in Levina and Bickel [17]. The local tangent space kernel bandwidth ϵ_N is estimated using the algorithm of Joncas et al. [14] for molecular dynamics data. Parameters are summarized in Table 1. Experiments were performed in Python on a 16 core Linux Debian Cluster with 768 gigabytes of RAM. Code is available at github.com/codanonymous/tslasso. Data is available at <https://figshare.com/s/fbd95c10b09f1140389d>.

Dataset	n	N_a	D	d	ϵ_N	n'	p	ω
Eth	50000	9	50	2	3.5	100	12	25
Mal	50000	9	50	2	3.5	100	12	25
Tol	50000	15	50	1	1.9	100	30	25

Table 1: Parameters in different experiments: Eth (Ethanol), Mal (Malonaldehyde) and Tol (Toluene)

These simulations dynamically generate atomic configurations which, due to interatomic interactions, exhibit non-linear, multiscale, non-i.i.d. noise, as well as non-trivial topology and geometry. That is, they lie near a low-dimensional manifold [9]. Such simulations are reasonable application for TSLASSO because there is no sparse parameterization of the data manifold known a priori. Such parameterizations are useful. They provide scientific insight about the data generating mechanism, and can be used to bias future simulations. However, these parameterizations are typically are detected by a trained human expert manually inspecting embedded data manifolds for covariates of interest. Therefore, we instead apply TSLASSO to identify functional covariates that parameterize this manifold.

Experiment Setups We obtain a Euclidean group-invariant featurization of the atomic coordinates as a vector of planar angles $a_i \in \mathbb{R}^{3\binom{N_a}{3}}$: the planar angles formed by triplets of atoms in the molecule [7]. We then perform an SVD on this featurization, and project the data onto the top $D = 50$ singular vectors to remove linear redundancies. Note that this represents a particular metric on the molecular *shape space*.

The dictionaries we considered are constructed on *bond diagram*, a priori information about molecular structure garnered from historical work. Building a dictionary based on this structure is akin to many other methods in the field [15, 27]. Specifically, this dictionary consist of all equivalence classes of 4-tuples of atoms implicitly defined along the molecule skeletons.

Since original angular data featurization is an overparameterization of the shape space, one cannot use automatically obtained gradients in TSLASSO. We therefore project the gradients prior to normalization on the tangent bundle of the shape space as it is embedded in \mathbb{R}^D .

For TSLASSO, the regularization parameter λ_n ranges from 0 to the value for which $\|\mathbf{B}_{\cdot j}\|_2 = 0$ for all j . The last d surviving dictionary functions are chosen as the parameterization for the manifold.

Results on MDS Data The toeune case is a manifold with $d = 1$. We observe that in all replicates, TSLASSO successfully select one of the six torsions associated with the peripheral methyl group bond, which shows the ability of our algorithm to automatically select appropriate parametrizing functions.

We plot the incoherence for Ethanol and Malonaldehyde as the heatmap in figure 2b and 2f, which present two groups of highly linearly dependent torsions, corresponding to the two bonds between heavy atoms in the molecules. Therefore, we expect to select a pair of incoherent torsions out of these dictionaries. In figure 2h and 2d, support recovery frequencies for sets of size $d = s = 2$ using TSLASSO on ethanol and malonaldehyde data respectively. As we expected, TSLASSO select one function from the two groups of highly colinear functions in most replicates. These results shows that our approach is able to identify embedding coordinates that are comparable or preferable to the a priori known functional support.

Results such as these usually are generated subsequent to running a non-parametric manifold learning algorithm, either through visual or saliency-based analyses, but we are able to achieve comparable results without the use of such an algorithm. See supplementary materials for a comparison of our algorithm with other manifold learning algorithms. These results also suggest that the local denoising property of the tangent space estimation, coupled with the global regularity imposed by the assumption that the manifold is parameterized by the same functions throughout, is sufficient to replicate the denoising effect of a manifold learning algorithm. Plus, with the help of domain functions, our embeddings come with good interpretability.

Also we point out that in our experiments, the subsampled size $n' = 100$ is only around 1% of the whole dataset and in almost all replicates this subsample is sufficient to obtain a valid parametrization. Tangent space estimation is only needed for these points. Therefore bypassing the usual manifold embedding procedure (on the whole dataset) we are able to obtain interpretable embeddings with fewer samples and in a shorter time.

6 Discussion and Related Work

Our method has several good properties. As long as the dictionary is constructed from some functions that have meaning in the domain of the problem, then our learned embedding is *interpretable* by definition. Furthermore, as discussed in Section 2, the mapping f_S is smooth, (implicitly) invertible, and can be naturally extended to values $\xi \in \mathcal{M}$ not in the data. Finally, our method is flexible with respect to a range of non-linearities.

These features contrast with standard approaches in non-linear dimension reduction. Parametrizing high-dimensional data by a small subset of smooth functions has been studied outside the context of manifold learning as *autoencoders* [11]. Early work on parametric manifold learning includes Saul and Roweis [22] and Teh and Roweis [24], who proposed a mixture of local linear models whose coordinates are aligned. In a *non-parametric* setting, LTSA [31] also gives a global parametrization by aligning locally estimated tangent spaces. When principal eigenvectors of the Laplace-Beltrami operator on the manifold are used for embedding, like in Diffusion Maps [8], it can be shown [20] that in the limit of large n , with properly selected eigenfunctions and geometric conditions on the manifold, the eigenfunctions provide a smooth embedding of the manifold to Euclidean space. However, both the parametric and non-parametric methods above produce learned embeddings f that are abstract in the sense that they do not have a concise functional form. In this sense, we draw a parallel between our approach and *factor models* [28].

Group Lasso type regression for gradient-based variable selection was previously explored in Haufe et al. [12] and Ye and Xie [29], but both have a simpler group structure, and are not utilized in the setting of dimension reduction. More recently, so-called *symbolic regression* methods such as Brunton et al. [4], Rudy et al. [21], and Champion et al. [5] have been used for linear, non-linear, and machine-learned systems, respectively, and these methods may regarded as univariate relatives of our

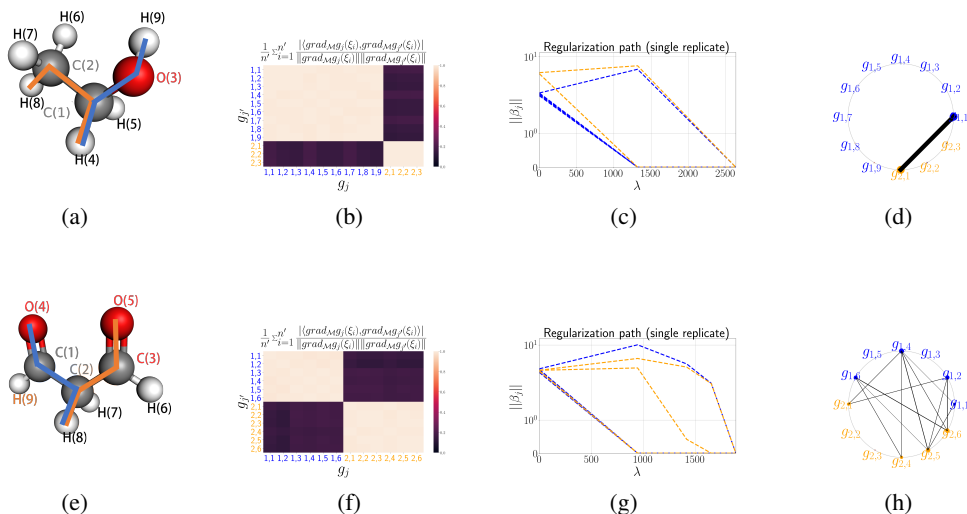


Figure 2: Results from molecular dynamics data. 2a, 2e show bond diagrams for ethanol and malonaldehyde, respectively. 2b and 2f show the heatmap of cosines (incoherences) of dictionary functions. The color is darker when there is more colinearity. 2c, 2g are regularization paths for a single replicate of ethanol and malonaldehyde. Note that in both figures there are a redundant trajectory of two functions that are added together. 2d, 2h Selection of pairs of functions for ethanol and malonaldehyde over replicants using TSLASSO . The node point on the circles represents all functions in the dictionary and the number along the lines are frequencies of each pairs selected over 25 repetitions. 2d means in all 25 repetitions, TSLASSO selects $g_{1,1}$ and $g_{2,1}$, which are the bond torsions around C-C bond and C-O bond respectively. 2h show that in 24 out of 25 replicates, TSLASSO is able to select one function from each highly colinear function group.

approach, since they are concerned with dynamics through time, while we consider the data manifold independently of time.

We also draw several distinctions between the TSLASSO method and the MANIFOLDLASSO method in Meila et al. [18]. First, MANIFOLDLASSO uses the same essential idea of sparse linear regression in gradient space, but in order to explain individual embedding coordinate functions. In contrast, we have no consistent matching between unit vectors in \mathbf{I}_d , and so can only provide an overall regularization path, rather than one corresponding to individual tangent basis vectors. The tangent bases are not themselves gradients of a known function, and, indeed it may not be the case that such a function even exists. Second, TSLASSO method dispenses with the entire *Embedding algorithm*, Riemannian metric estimation, and pulling back the embedding gradients steps in MANIFOLDLASSO, while providing almost everything a user can get from MANIFOLDLASSO. Apart from simplification, TSLASSO can be run on $n' \ll n$ data points, about 1/500 of the data in our experiments (Table 1), while the algorithm in MANIFOLDLASSO computes an embedding from all data points. Hence, all operations before the actual GroupLasso are hundreds of times faster than in MANIFOLDLASSO. Theoretically, Meila et al. [18] only provides (i) analysis in function spaces, and (ii) recovery guarantees for the final step, GroupLasso, based on generic assumptions about the noise. Our paper has end-to-end guarantees of recovery guarantees from a sample in Section 4.

The reliance on domain prior knowledge in the form of the dictionary \mathcal{F} is essential for TSLASSO, and can be a restriction to its usability in practice, especially given the restrictions on gradient field colinearity. However, as the experiments have illustrated, there are domains where construction of a dictionary is reasonable, and explaining the behavior of organic molecules in terms of torsions and planar angles is common in chemistry and drug design [2, 13]. More generally, it would be desirable to utilize a completely agnostic dictionary that also contained the features themselves, and so development of an optimization strategy capable of handling the large amount of colinearity intrinsic to such a set-up is an active area of research.

Acknowledgement

The authors acknowledge the support from NSF DMS award 1810975 and DMS award 2015272. The authors also thank the Tkatchenko lab, and especially Stefan Chmiela for providing both data and expertise. This work is completed at the Pure and Applied Mathematics (IPAM). Marina also gratefully acknowledges a Simons Fellowship from IPAM to her, which made her stay during Fall 2019 possible.

References

- [1] Eddie Aamari and Clément Levrard. Stability and minimax optimality of tangential delaunay complexes for manifold reconstruction. *Discrete & Computational Geometry*, 59(4):923–971, 2018. doi: 10.1007/s00454-017-9962-z. URL <https://doi.org/10.1007/s00454-017-9962-z>.
- [2] Matthew A. Addicoat and Michael A. Collins. Potential energy surfaces: the forces of chemistry. In Mark Brouard and Claire Vallance, editors, *Tutorials in Molecular Reaction Dynamics*, chapter 2, pages 28–49. Royal Society of Chemistry Publishing, London, 2010.
- [3] M. Belkin and P. Niyogi. Laplacian eigenmaps and spectral techniques for embedding and clustering. In *Advances in Neural Information Processing Systems 14*, Cambridge, MA, 2002. MIT Press.
- [4] Steven L. Brunton, Joshua L. Proctor, and J. Nathan Kutz. Discovering governing equations from data by sparse identification of nonlinear dynamical systems. *Proceedings of the National Academy of Sciences*, 113(15):3932–3937, 2016. ISSN 0027-8424. doi: 10.1073/pnas.1517384113. URL <http://www.pnas.org/content/113/15/3932>.
- [5] Kathleen Champion, Bethany Lusch, J Nathan Kutz, and Steven L Brunton. Data-driven discovery of coordinates and governing equations. *Proc. Natl. Acad. Sci. U. S. A.*, 116(45):22445–22451, November 2019.
- [6] Guangliang Chen, Anna V. Little, and Mauro Maggioni. *Multi-Resolution Geometric Analysis for Data in High Dimensions*, pages 259–285. Birkhäuser Boston, Boston, 2013. ISBN 978-0-8176-8376-4. doi: 10.1007/978-0-8176-8376-4-13. URL <https://doi.org/10.1007/978-0-8176-8376-4-13>.
- [7] Yu-Chia Chen, James McQueen, Samson J. Koelle, Marina Meila, Stefan Chmiela, and Alexandre Tkatchenko. Modern manifold learning methods for md data – a step by step procedural overview. www.stat.washington.edu/mmp/Papers/mlcules-arxiv.pdf, July 2019.
- [8] R. R. Coifman, S. Lafon, A. Lee, Maggioni, Warner, and Zucker. Geometric diffusions as a tool for harmonic analysis and structure definition of data: Diffusion maps. In *Proceedings of the National Academy of Sciences*, pages 7426–7431, 2005.
- [9] P. Das, M. Moll, H. Stamati, L.E. Kavraki, and C. Clementi. Low-dimensional, free-energy landscapes of protein-folding reactions by nonlinear dimensionality reduction. *Proceedings of the National Academy of Sciences*, 103(26):9885–9890, 2006.
- [10] Mojtaba Kadkhodaie Elyaderani, Swayambhoo Jain, Jeffrey Druce, Stefano Gonella, and Jarvis Haupt. Group-level support recovery guarantees for group lasso estimator. pages 4366–4370, 2017. doi: 10.1109/ICASSP.2017.7952981.
- [11] Ian Goodfellow, Yoshua Bengio, and Aaron Courville. *Deep Learning*. MIT Press, 2016. <http://www.deeplearningbook.org>.
- [12] Stefan Haufe, Vadim V Nikulin, Andreas Ziehe, Klaus-Robert Müller, and Guido Nolte. Estimating vector fields using sparse basis field expansions. In D Koller, D Schuurmans, Y Bengio, and L Bottou, editors, *Advances in Neural Information Processing Systems 21*, pages 617–624. Curran Associates, Inc., 2009.

- [13] Bing Huang and O Anatole von Lilienfeld. Communication: Understanding molecular representations in machine learning: The role of uniqueness and target similarity. *J. Chem. Phys.*, 145(16):161102, October 2016.
- [14] Dominique Joncas, Marina Meila, and James McQueen. Improved graph laplacian via geometric Self-Consistency. In I Guyon, U V Luxburg, S Bengio, H Wallach, R Fergus, S Vishwanathan, and R Garnett, editors, *Advances in Neural Information Processing Systems 30*, pages 4457–4466. Curran Associates, Inc., 2017.
- [15] Mario Krenn, Florian Häse, Akshatkumar Nigam, Pascal Friederich, and Alan Aspuru-Guzik. Self-referencing embedded strings (SELFIES): A 100% robust molecular string representation. *Mach. Learn.: Sci. Technol.*, 1(4):045024, October 2020.
- [16] John M. Lee. *Introduction to Smooth Manifolds*. Springer-Verlag New York, 2003.
- [17] Elizaveta Levina and Peter J. Bickel. Maximum likelihood estimation of intrinsic dimension. In *Advances in Neural Information Processing Systems 17 NIPS 2004, December 13-18, 2004, Vancouver, British Columbia, Canada*, pages 777–784, 2004. URL <http://papers.nips.cc/paper/2577-maximum-likelihood-estimation-of-intrinsic-dimension>.
- [18] Marina Meila, Samson Koelle, and Hanyu Zhang. A regression approach for explaining manifold embedding coordinates. *arXiv e-prints*, art. arXiv:1811.11891, Nov 2018.
- [19] Guillaume Obozinski, Martin J. Wainwright, and Michael I. Jordan. Support union recovery in high-dimensional multivariate regression. *The Annals of Statistics*, 39(1):1–47, 2011. ISSN 00905364. URL <http://www.jstor.org/stable/29783630>.
- [20] Jacobus W Portegies. Embeddings of Riemannian manifolds with heat kernels and eigenfunctions. *Communications on Pure and Applied Mathematics*, 69(3):478–518, 2016.
- [21] Samuel Rudy, Alessandro Alla, Steven L Brunton, and J Nathan Kutz. Data-Driven identification of parametric partial differential equations. *SIAM J. Appl. Dyn. Syst.*, 18(2):643–660, January 2019.
- [22] Lawrence K. Saul and Sam T. Roweis. Think globally, fit locally: Unsupervised learning of low dimensional manifolds. *J. Mach. Learn. Res.*, 4:119–155, December 2003. ISSN 1532-4435. doi: 10.1162/153244304322972667. URL <https://doi.org/10.1162/153244304322972667>.
- [23] A. Singer and H.-T. Wu. Vector diffusion maps and the connection laplacian. *Communications on Pure and Applied Mathematics*, 65(8):1067–1144, 2012. doi: <https://doi.org/10.1002/cpa.21395>. URL <https://onlinelibrary.wiley.com/doi/abs/10.1002/cpa.21395>.
- [24] Yee Whye Teh and Sam T. Roweis. Automatic alignment of local representations. In *NIPS*, 2002.
- [25] Laurens van der Maaten and Geoffrey Hinton. Visualizing data using t-sne. *Journal of Machine Learning Research*, 9:2579–2605, Nov 2008.
- [26] Martin J. Wainwright. Sharp thresholds for high-dimensional and noisy sparsity recovery using ℓ_1 -constrained quadratic programming (lasso). *IEEE Transactions on Information Theory*, 55: 2183–2202, 2009.
- [27] Tian Xie, Arthur France-Lanord, Yanming Wang, Yang Shao-Horn, and Jeffrey C Grossman. Graph dynamical networks for unsupervised learning of atomic scale dynamics in materials. *Nat. Commun.*, 10(1):2667, June 2019.
- [28] Ilker Yalcin and Yasuo Amemiya. Nonlinear factor analysis as a statistical method. *Statist. Sci.*, 16(3):275–294, 08 2001. doi: 10.1214/ss/1009213729. URL <https://doi.org/10.1214/ss/1009213729>.
- [29] Gui-Bo Ye and Xiaohui Xie. Learning sparse gradients for variable selection and dimension reduction. *Machine Learning*, 87(3):303–355, Jun 2012. ISSN 1573-0565. doi: 10.1007/s10994-012-5284-9. URL <https://doi.org/10.1007/s10994-012-5284-9>.

- [30] M Yuan and Y Lin. Model selection and estimation in regression with grouped variables. *J. R. Stat. Soc. Series B Stat. Methodol.*, 2006.
- [31] Zhenyue Zhang and Hongyuan Zha. Principal manifolds and nonlinear dimensionality reduction via tangent space alignment. *SIAM J. Scientific Computing*, 26(1):313–338, 2004.

Supplementary Materials

A Proofs

In this section we will provide proofs to the theoretical results in the main text.

A.1 Independence of Tangent Basis Selection

Proposition A.1. *Consider alternative bases $\mathbf{T}'_i = \mathbf{T}_i \mathbf{\Gamma}_i$ where $\mathbf{\Gamma}_i$ are $d \times d$ orthonormal matrices. If $\{\mathbf{B}_i\}_{i=1}^n$ minimizes (4), then in the new tangent bases, $\{\mathbf{B}_i \mathbf{\Gamma}_i\}_{i=1}^n$ minimizes the corresponding loss function, which is constructed through replacing \mathbf{X}_i by $\mathbf{\Gamma}_i \mathbf{X}_i$ in (4). Furthermore, the selected support S is independent of the basis chosen for each tangent space.*

Proof of Proposition 2. It suffices to show that the loss in (4) does not change under orthogonal transformation of individual tangent bases. As long as this holds, $\mathbf{B}_i \mathbf{\Gamma}_i$ must minimize the loss since otherwise one could argue that $J_{\lambda_n}(\mathbf{B})$ is not a minimum value for the original tangent space bases. Note that the norm $\|\mathbf{B}_{\cdot j}\|_2$ is unitary invariant. This is because $\mathbf{B}_{\cdot j} = (j\text{-th row of } \mathbf{B}_i)_{i=1}^n$ is constructed by stacking the j -th row of each \mathbf{B}_i . Hence the new norm is given by the norm of $(j\text{-th row of } \mathbf{B}_i \mathbf{\Gamma}_i)_{i=1}^n$; therefore the Group Lasso penalty doesn't change after changing \mathbf{B}_i to $\mathbf{B}_i \mathbf{\Gamma}_i$ for each i . Finally, it holds that $\|\mathbf{I}_d - \mathbf{\Gamma}_i^\top \mathbf{X}_i \mathbf{B}_i \mathbf{\Gamma}_i\|_F^2 = \|\mathbf{\Gamma}_i^\top (\mathbf{I}_d - \mathbf{X}_i \mathbf{B}_i) \mathbf{\Gamma}_i\|_F^2 = \|\mathbf{I}_d - \mathbf{X}_i \mathbf{B}_i\|_F^2$, so the ℓ_2 -loss is not changed under orthonormal transformation of the tangent bases. These rotation invariances guarantee the same support S . \square

A.2 Proof of Proposition 3

We start by stating the following lemma, which gives the sufficient and necessary condition of certain matrices \mathbf{B}_i to be the solution to problem (4). It also provides conditions on unique support recovery and unique solutions. The proof is standard in convex analysis literature; we follow a procedure as in [26].

Lemma A.2. *1. Matrix \mathbf{B} is the optimal solution to problem (4) if and only if there exists an matrix $\mathbf{Z} = (z_1^\top, z_2^\top, \dots, z_p^\top)^\top \in \mathbb{R}^{p \times nd}$ such that*

$$z_j = \begin{cases} \frac{\beta_i}{\|\beta_i\|} & \beta_i \neq 0 \\ \in \mathbb{R}^{nd} \text{ with } \|z_j\|_2 \leq 1, & \text{otherwise} \end{cases} \quad (10)$$

and

$$(\mathbf{X}_1^\top (\mathbf{I}_d - \mathbf{X}_1 \mathbf{B}_1), \mathbf{X}_2^\top (\mathbf{I}_d - \mathbf{X}_2 \mathbf{B}_2), \dots, \mathbf{X}_n^\top (\mathbf{I}_d - \mathbf{X}_n \mathbf{B}_n)) = \frac{\lambda_n}{\sqrt{nd}} \mathbf{Z} \quad (11)$$

2. *If under the setting of (a), further in (10), we have $\|z_i\| < 1$ whenever $\beta_i = 0$, then all optimal solutions $\tilde{\mathbf{B}}$ of problem (4) will have support $S(\tilde{\mathbf{B}}) \subset S(\mathbf{B})$.*
3. *Under setting of (a) and (b). Let $\mathbf{X}_{iS(\mathbf{B})}$ be the submatrix constructed by the $S(\mathbf{B})$ columns of \mathbf{X}_i . If all $\mathbf{X}_{iS(\mathbf{B})}^\top \mathbf{X}_{iS(\mathbf{B})}$ are invertible, then the solution of problem (4) is unique.*

Proof. Before we further explore the result, we transform the problem (4). We stack the matrices at each point together. We will now write

$$\mathbf{X} = \begin{pmatrix} \mathbf{X}_1 \\ \mathbf{X}_2 \\ \dots \\ \mathbf{X}_n \end{pmatrix} \in \mathbb{R}^{nd \times p}, \quad \mathbf{B} = (\mathbf{B}_1, \mathbf{B}_2, \dots, \mathbf{B}_n) \in \mathbb{R}^{p \times nd} \quad (12)$$

Then β_j is the j -th row for \mathbf{B} . Further let matrix

$$\mathbf{E}_i = (\mathbf{0}, \dots, \mathbf{0}, \mathbf{I}_d, \mathbf{0}, \dots, \mathbf{0})^\top \in \mathbb{R}^{nd \times d} \quad (13)$$

be the block matrix with the i -th block being identity matrix and the other blocks are all zeros. Then the loss function of TSLasso can be rewritten as

$$J_{\lambda_n}(\mathbf{B}) = \frac{1}{2} \sum_{i=1}^n \|\mathbf{E}_i^\top (\mathbf{I}_{nd} - \mathbf{X}\mathbf{B})\mathbf{E}_i\|_F^2 + \frac{\lambda_n}{\sqrt{nd}} \|\mathbf{B}\|_{1,2} \quad (14)$$

where $\|\mathbf{B}\|_{1,2}$ is the norm defined by $\sum_{j=1}^p \|\beta_j\|_2$.

The proof of this lemma is standard technique in convex analysis. Define $h_i(\mathbf{B}) = \|\mathbf{E}_i^\top (\mathbf{I}_{nd} - \mathbf{X}\mathbf{B})\mathbf{E}_i\|_F^2$ penalty part and g is the group lasso penalty.

The first step is to compute the gradient of $h_i(\mathbf{B})$ with respect to \mathbf{B} . For any $\mathbf{H} \in \mathbb{R}^{p \times nd}$, compute

$$h_i(\mathbf{B} + \mathbf{H}) - h_i(\mathbf{B}) \quad (15)$$

$$= \text{trace}(\mathbf{E}_i^\top (\mathbf{I}_{nd} - \mathbf{X}(\mathbf{B} + \mathbf{H}))\mathbf{E}_i)^\top (\mathbf{E}_i^\top (\mathbf{I}_{nd} - \mathbf{X}(\mathbf{B} + \mathbf{H}))\mathbf{E}_i) - \text{trace}(\mathbf{E}_i^\top (\mathbf{I}_{nd} - \mathbf{X}\mathbf{B})\mathbf{E}_i)^\top (\mathbf{E}_i^\top (\mathbf{I}_{nd} - \mathbf{X}\mathbf{B})\mathbf{E}_i) \quad (16)$$

$$= -2 \text{trace}(\mathbf{H}^\top \mathbf{X}^\top \mathbf{E}_i \mathbf{E}_i^\top (\mathbf{I}_{nd} - \mathbf{X}\mathbf{B})\mathbf{E}_i \mathbf{E}_i^\top) + O(\|\mathbf{H}\|_F^2) \quad (17)$$

$$= -2 \langle \mathbf{H}, \mathbf{X}^\top \mathbf{E}_i \mathbf{E}_i^\top (\mathbf{I}_{nd} - \mathbf{X}\mathbf{B})\mathbf{E}_i \mathbf{E}_i^\top \rangle_F + O(\|\mathbf{H}\|_F^2) \quad (18)$$

Hence we can conclude that $\nabla_{\mathbf{B}} h_i(\mathbf{B}) = -2\mathbf{X}^\top \mathbf{E}_i \mathbf{E}_i^\top (\mathbf{I}_{nd} - \mathbf{X}\mathbf{B})\mathbf{E}_i \mathbf{E}_i^\top = -2\mathbf{X}^\top \mathbf{E}_i (\mathbf{I}_d - \mathbf{X}_i \mathbf{B}_i) \mathbf{E}_i^\top$, and therefore

$$\begin{aligned} \nabla_{\mathbf{B}} \frac{1}{2} \sum_{i=1}^n \|\mathbf{I}_d - \mathbf{X}_i \mathbf{B}_i\|_F^2 &= \sum_{i=1}^n -\mathbf{X}^\top \mathbf{E}_i (\mathbf{I}_d - \mathbf{X}_i \mathbf{B}_i) \mathbf{E}_i^\top \\ &= -(\mathbf{X}_1^\top (\mathbf{I}_d - \mathbf{X}_1 \mathbf{B}_1), \mathbf{X}_2^\top (\mathbf{I}_d - \mathbf{X}_2 \mathbf{B}_2), \dots, \mathbf{X}_n^\top (\mathbf{I}_d - \mathbf{X}_n \mathbf{B}_n)). \end{aligned} \quad (19)$$

Recall that we use β_i to denote the i -th row of \mathbf{B} . We use a similar argument in proof of lemma 2 of [19] and notice that the original optimization problem is convex and strictly feasible (hence strong duality holds). The primal problem is

$$\min_{\substack{\mathbf{B} \in \mathbb{R}^{p \times nd} \\ b \in \mathbb{R}^p}} \frac{1}{2} \sum_{i=1}^n \|\mathbf{E}_i^\top (\mathbf{I}_{nd} - \mathbf{X}\mathbf{B})\mathbf{E}_i\|_F^2 + \frac{\lambda_n}{\sqrt{nd}} \sum_{j=1}^p b_j \quad (20)$$

$$s.t. (\beta_j, b_j) \in \mathcal{K}, 1 \leq j \leq p \quad (21)$$

where \mathcal{K} is the second-order cone as usually defined. The dual problem is given by

$$\max_{\substack{\mathbf{Z} \in \mathbb{R}^{p \times nd} \\ t \in \mathbb{R}^p}} \min_{\substack{\mathbf{B} \in \mathbb{R}^{p \times nd} \\ b \in \mathbb{R}^p}} L(\mathbf{B}, b, \mathbf{Z}, t) = \frac{1}{2} \sum_{i=1}^n \|\mathbf{E}_i^\top (\mathbf{I}_{nd} - \mathbf{X}\mathbf{B})\mathbf{E}_i\|_F^2 + \frac{\lambda_n}{\sqrt{nd}} \sum_{j=1}^p b_j + \sum_{j=1}^p \langle (z_j, t_j), (\beta_j, b_j) \rangle \quad (22)$$

$$s.t. (z_j, t_j) \in \mathcal{K}^\circ \quad (23)$$

where $z_j \in \mathbb{R}^{nd}$ is the j -th row of \mathbf{Z} . Note that \mathcal{K}° is the polar cone of \mathcal{K} and second order cone is self-dual. Hence we have $(z_i, -\mathbf{T}_i) \in \mathcal{K}$.

Since the primal problem is strictly feasible, strong duality holds. For any pair of (\mathbf{B}^*, b^*) and (\mathbf{Z}^*, t^*) primal and dual solutions, they have to satisfy the KKT condition that

$$\|\beta_j^*\|_2 \leq b_j^*, \quad 1 \leq j \leq p, \quad (24a)$$

$$\|z_j^*\|_2 \leq -t_j^*, \quad 1 \leq j \leq p, \quad (24b)$$

$$z_j^{*T} \beta_j^* + t_j^* b_j^* = 0, \quad 1 \leq j \leq p, \quad (24c)$$

$$\nabla_{\mathbf{B}} \left[\frac{1}{2} \sum_{i=1}^n \|\mathbf{I}_d - \mathbf{X}_i \mathbf{B}_i\|_F^2 \right] + \mathbf{Z}^* = 0, \quad (24d)$$

$$\frac{\lambda_n}{\sqrt{nd}} + t_j^* = 0. \quad (24e)$$

Note that (24c) implies that $t_j^* = -\frac{\lambda_n}{\sqrt{nd}}$. Then by (24a) and (24b) we have $\|z_j^{*T} \beta_j^*\| \leq \frac{\lambda_n}{\sqrt{nd}} \|\beta_j\|_2$. Notice that the equality holds in (24c), there fore $\|z_j^*\| = \frac{\sqrt{nd}}{\lambda_n}$ and $b_j^* = \|\beta_j^*\|$. Renormalize $z_j^* = \frac{\sqrt{nd}}{\lambda_n} z_j^*$ and part (a) holds. For part b, for any j , $z_j^{*T} \beta_j = \|\beta_j\|_2$. Then $\beta_j = 0$ must hold for any $\|z_j\| < 1$. For part (c) note that in this case the loss function is strictly convex when the original problem is restricted to minimizing over $\mathbf{B} : \beta_i = 0, \quad \forall i \notin S(\mathbf{B})$. This strict convexity implies the uniqueness of solution. \square

The previous lemma provides a tool for understanding the support recovery consistency of TSLASSO. For any arbitrary $S \subset [p]$ such that $|S| = d$, $\text{rank } \mathbf{X}_{iS} = d$ holds for all $i \in [n]$, we establish a sufficient condition on \mathbf{X}_{iS} such that they can be discovered by the TSLASSO. Suppose at each data point i , we decompose the matrix \mathbf{I}_d by

$$\mathbf{I}_d = \mathbf{X}_{iS} \mathbf{B}_{iS}^* + \mathbf{W}_{iS} \quad (25)$$

where \mathbf{B}_{iS}^* are $p \times d$ matrices that only has non zero entries in rows in S and minimizes the loss $\|\mathbf{I}_d - \mathbf{X}_i \mathbf{B}_i\|_F^2$. In fact, since \mathbf{X}_{iS} is full rank, there exists a unique \mathbf{B}_{iS}^* for each i such that $\mathbf{W}_{iS} = 0$. Denote $\mathbf{B}_{i,j}^*$ be the j -th row in \mathbf{B}_{iS}^* and define

$$\tilde{b}_S = \min_{i \in [n]} \min_{j \in S} \|\mathbf{B}_{i,j}^*\|, \quad (26)$$

This is a sample version of b_S defined in (5).

The following lemma shows a sufficient condition on \mathbf{X}_i so that the true support can be found. We first define several derived quantities of \mathbf{X}_i . Denoting the j -th column of matrix \mathbf{X}_i by x_{ij} , we define

$$\text{S-incoherence} \quad \tilde{\mu}_S = \max_{i=1:n, j \in S, j' \notin S} \frac{|x_{ij}^\top x_{ij'}|}{\|\nabla f_j(\xi_i)\| \|\nabla f_{j'}(\xi_i)\|} \quad (27a)$$

$$\text{internal-collinearity} \quad \tilde{\nu}_S = \max_{\beta=1:n} \|(\tilde{\mathbf{X}}_{iS}^\top \tilde{\mathbf{X}}_{iS})^{-1} - \mathbf{G}_S(\xi_i)^2\|. \quad (27b)$$

$$\text{maximal gradient norm} \quad \tilde{\phi}_S = \max_{i=1:n} \max_{j \in S} \|\nabla f_j(\xi_i)\| \quad (27c)$$

These are sampled version of μ_S, ν_S and ϕ_S defined on the whole manifold from (6), (7) and (8).

Now we are ready to prove proposition 4.2. We start with some lemmas in linear algebra.

Lemma A.3. Let \mathbf{A}, \mathbf{B} be $d \times d$ positive definite matrices. Then $\|\mathbf{A}^{-1} - \mathbf{B}^{-1}\| \leq \|\mathbf{B}^{-1}\|^2 \|\mathbf{A} - \mathbf{B}\|$

Lemma A.4. Let \mathbf{A}, \mathbf{B} be two $d \times d$ matrices. \mathbf{A} is positive semidefinite. Denote $\|\mathbf{A}\|_{\infty, 2}$ be the maximum ℓ_2 norm of the rows of \mathbf{A} . Then $\|\mathbf{AB}\|_{\infty, 2} \leq \|\mathbf{A}\| \|\mathbf{B}\|_F$

Proof. Write $\mathbf{A} = (a_{ij})_{d \times d}$, $\mathbf{B} = (b_{ij})_{d \times d}$, then by definition

$$\begin{aligned} \|\mathbf{AB}\|_{\infty, 2}^2 &= \max_{i=1:d} \sum_{j=1}^d \left(\sum_{k=1}^d a_{ik} b_{kj} \right)^2 \\ &\leq \max_{i=1:d} \sum_{j=1}^d \left(\sum_{k=1}^d a_{ik}^2 \right) \left(\sum_{k=1}^d b_{kj}^2 \right) \\ &\leq \left(\max_{i=1:d} \sum_{k=1}^d a_{ik}^2 \right) \left(\sum_{j=1}^d \sum_{k=1}^d b_{kj}^2 \right) \\ &= \|\mathbf{A}\|_{\infty, 2}^2 \|\mathbf{B}\|_F^2. \end{aligned}$$

Since \mathbf{A} is positive semidefinite, we have

$$\|\mathbf{A}\|_{\infty, 2}^2 = \max_{i=1:d} (\mathbf{AA})_{ii} \leq \|\mathbf{A}^2\| = \|\mathbf{A}\|^2.$$

Hence we conclude the desired result. \square

Lemma A.5. Let $\delta = \min_{\xi \in \mathcal{M}} \min_{j=1:p} \|\nabla f_j(\xi)\|$, then $\|(\mathbf{X}_{iS}^\top \mathbf{X}_{iS})^{-1}\|_2 \leq 1 + \frac{\tilde{\nu}_S}{\delta^2}$

Proof. Recall that $\mathbf{G}_S(\xi_i) = \text{diag}\{\|\nabla f_j(\xi_i)\|\}_{j,j' \in S}$. We first consider that

$$\|(\mathbf{X}_{iS}^\top \mathbf{X}_{iS})^{-1} - \mathbf{I}_d\|_2 \quad (28)$$

$$= \|\mathbf{G}_S^{-1}(\xi_i)(\tilde{\mathbf{X}}_{iS}^\top \tilde{\mathbf{X}}_{iS})^{-1} \mathbf{G}_S(\xi_i)^{-1} - \mathbf{G}_S^{-1}(\xi_i) \mathbf{G}_S(\xi_i)^2 \mathbf{G}_S^{-1}(\xi_i)\| \quad (29)$$

$$\leq \|(\tilde{\mathbf{X}}_{iS}^\top \tilde{\mathbf{X}}_{iS})^{-1} - \mathbf{G}_S(\xi_i)^2\| \|\mathbf{G}_S^{-1}(\xi_i)\|^2 \quad (30)$$

$$\leq \frac{\tilde{\nu}_S}{\delta^2} \quad (31)$$

And the desired results come from triangular inequality. \square

Lemma A.6. Let $\{\xi_i\}_{i=1}^n$ be fixed data points on \mathcal{M} . Let $\tilde{\delta} = \min_{\xi \in \mathcal{M}} \min_{j=1:p} \|\nabla f_j(\xi)\|$ and $\Gamma = \max_{\xi \in \mathcal{M}} \max_{j=1:p} \|\nabla f_j(\xi)\|$. Let $\tilde{\mu}_S, \tilde{\nu}_S, \tilde{\phi}_S$ defined from \mathbf{X}_{iS} according to (27a), (27b) and (27c) respectively. Then Tangent Lasso problem (4) has a unique solution $\hat{\mathbf{B}} = [\hat{\mathbf{B}}_1, \hat{\mathbf{B}}_2, \dots, \hat{\mathbf{B}}_n] \in \mathbb{R}^{p \times nd}$ with support $S(\hat{\mathbf{B}})$ included in the true support S if $(1 + \frac{\tilde{\nu}_S}{\delta^2})^2 \tilde{\mu}_S \tilde{\phi}_S \Gamma d < 1$. Furthermore, if $\lambda_n(1 + \tilde{\nu}_S/\delta^2)^2 < \tilde{b}_S \sqrt{n}/2$, then $S(\hat{\mathbf{B}}) = S$.

Proof. We follow the procedure of Primal-Dual witness method (see e.g. Wainwright [26], Obozinski et al. [19], Elyaderani et al. [10]).

Still considering the reformulated optimization problem (14), we first find $\hat{\mathbf{B}}$ from minimizing a restricted optimization problem

$$\min_{S(\mathbf{B}) \subset S} J_{\lambda_n}(\mathbf{B}) = \frac{1}{2} \sum_{i=1}^n \|\mathbf{E}_i^\top (\mathbf{I}_{nd} - \mathbf{X}\mathbf{B}) \mathbf{E}_i\|_F^2 + \frac{\lambda_n}{\sqrt{nd}} \|\mathbf{B}\|_{1,2}. \quad (32)$$

We then construct a dual solution $\hat{\mathbf{Z}}$ and show that $\hat{\mathbf{B}}$ is the solution to the original optimization problem. We write z_j as the j -th row of $\hat{\mathbf{Z}}$ and decompose each $\hat{z}_j = [\hat{z}_{j,1}, \hat{z}_{j,2}, \dots, \hat{z}_{j,n}]$. According to lemma A.2, we can solve for $\hat{\mathbf{Z}}$ from those optimality conditions.

First, notice that

$$\hat{\mathbf{B}}_{iS} - \mathbf{B}_{iS}^* = -\frac{\lambda_n}{\sqrt{nd}} (\mathbf{X}_{iS}^\top \mathbf{X}_{iS})^{-1} \hat{\mathbf{Z}}_{S,i}. \quad (33)$$

where $\hat{\mathbf{Z}}_S$ is constructed by concatenating the $j \in S$ row of $\hat{\mathbf{Z}}_i$.

For an $d \times d$ matrix \mathbf{A} , we write $\|\mathbf{A}\|_{\infty,2} = \max_{i=1}^d \|a_i\|_2$, where a_i is the i -th row of \mathbf{A} . Then it holds that from lemma A.4

$$\|(\mathbf{X}_{iS}^\top \mathbf{X}_{iS})^{-1} \hat{\mathbf{Z}}_{S,i}\|_{\infty,2} \leq \|(\mathbf{X}_{iS}^\top \mathbf{X}_{iS})^{-1}\| \|\hat{\mathbf{Z}}_{S,i}\|_F. \quad (34)$$

Therefore recall that $\|\hat{\mathbf{Z}}_S\|_{\infty,2} = 1$ we conclude that $\|\hat{\mathbf{Z}}_{S,i}\|_F \leq \sqrt{d}$. And adopting lemma A.5 we have

$$\|(\mathbf{X}_{iS}^\top \mathbf{X}_{iS})^{-1} \hat{\mathbf{Z}}_{S,i}\|_{\infty,2} \leq \sqrt{d} (1 + \frac{\tilde{\nu}_S}{\delta^2})^2 \quad (35)$$

According to (33) and the assumption, $\lambda_n \sqrt{d} (1 + \frac{\tilde{\nu}_S}{\delta^2})^2 / \sqrt{nd} < \frac{1}{2} \tilde{b}_S$, then $\|\hat{\mathbf{B}}_{iS,j}\| \geq \frac{1}{2} \tilde{b}_S$ for each row $j \in S$.

On the other hand, for any $j' \notin S$, we have

$$\hat{z}_{j',i} = x_{ij'}^\top \mathbf{X}_{iS} (\mathbf{X}_{iS}^\top \mathbf{X}_{iS})^{-1} \hat{\mathbf{Z}}_{S,i}. \quad (36)$$

It suffices to verify that $\|\hat{z}_j\| < 1$ for all $j' \notin S$. For any i , we have

$$\|x_{ij'}^\top \mathbf{X}_{iS} (\mathbf{X}_{iS}^\top \mathbf{X}_{iS})^{-1}\|_2 \leq (1 + \frac{\tilde{\nu}_S}{\delta^2})^2 \|x_{ij'}^\top \mathbf{X}_{iS}\|_2 \leq \sqrt{d} (1 + \frac{\tilde{\nu}_S}{\delta^2})^2 \tilde{\mu}_S \|\nabla f_{j'}(\xi_i)\| \max_{j \in S} \|\nabla f_j(\xi_i)\| \leq \sqrt{d} (1 + \frac{\tilde{\nu}_S}{\delta^2})^2 \tilde{\mu}_S \tilde{\phi}_S \Gamma \quad (37)$$

Directly compute that

$$\begin{aligned}
\|\hat{z}_{j'}\|^2 &\leq \sum_{i=1}^n \|x_{ij'}^\top \mathbf{X}_{iS} (\mathbf{X}_{iS}^\top \mathbf{X}_{iS})^{-1} \hat{\mathbf{Z}}_{S,i}\|_2^2 \\
&\leq \sum_{i=1}^n \|x_{ij'}^\top \mathbf{X}_{iS} (\mathbf{X}_{iS}^\top \mathbf{X}_{iS})^{-1}\|_2^2 \|\hat{\mathbf{Z}}_{S,i}\|_F^2 \\
&\leq d(1 + \frac{\tilde{\nu}_S}{\delta^2})^4 \tilde{\mu}_S^2 \tilde{\phi}_S^2 \Gamma^2 \sum_{i=1}^n \|\hat{\mathbf{Z}}_{S,i}\|_F^2 \\
&\leq (1 + \frac{\tilde{\nu}_S}{\delta^2})^4 \tilde{\mu}_S^2 \tilde{\phi}_S^2 \Gamma^2 d^2 < 1
\end{aligned}$$

□

This lemma is the recovery result if the tangent space is estimated without any noise. Note that this conditions also implies further results on the 'isometric' property of TSLasso. If there are two different subsets S, S' such that $|S| = |S'| = d$ and both has rank d at each data point. Then for both subsets, $\mathbf{X}_{iS}^\top \mathbf{X}_{iS}$ are invertible, and the lemma also implies that $\tilde{\mu}_S \tilde{\nu}_S d < 1$ cannot hold at the same time for both subsets. The one picked by TSLasso (usually) has a lower value of $\tilde{\nu}_S$, and will be closer to isometry to some extent.

This recovery result does not involve the tuning parameter for false inclusion. Therefore, it justifies our selection of tuning parameter that force the support has cardinality less than d . If we do observe d functions selected and they have rank d everywhere, then under incoherence condition they must be a right parameterization. To avoid false exclusion, the tuning parameter λ_n cannot be too large.

Now we connect these support recovery results inherent to our optimization approach with the tangent space estimation algorithm. Let $\mathbf{T}_i, \hat{\mathbf{T}}_i$ be the orthogonal basis in $\mathbb{R}^{D \times d}$ for true and estimated tangent space respectively, and write

$$e = \max_{i=1}^n \|\mathbf{T}_i \mathbf{T}_i^\top - \hat{\mathbf{T}}_i \hat{\mathbf{T}}_i^\top\|_2. \quad (38)$$

We have the following recovery result in the setting that gradient is estimated with some noise.

Lemma A.7. *Let $\xi_i, i = 1 : n$ be fixed data points on manifold $\mathcal{M} \subset \mathbb{R}^D$. Given S a subset of functions in dictionary $\mathcal{F} = \{f_j, j \in [p]\}$ with $|S| = d$. Suppose $\text{rank grad } f_S = d$ at each data point. Fix \mathbf{T}_i as an orthonormal basis of tangent space at ξ_i , and $\hat{\mathbf{T}}_i$ a basis for the estimated tangent space. And further define $\mathbf{X}_i = \mathbf{T}_i^\top [\nabla f_j]$, $\hat{\mathbf{X}}_i = \hat{\mathbf{T}}_i^\top [\nabla f_j]$, $j \in [p]$ where ∇ is the ambient gradient. Define $\mathbf{B}_{iS}^*, \tilde{b}_S$ the same as lemma A.6. Assume that $\|\nabla f_j\| = 1$ for all $\xi_i, i \in [n], j \in [p]$. Define $\tilde{\mu}_S, \tilde{\nu}_S$ from (27a) and (27b) and e from (38). Then let $\hat{\mathbf{B}}$ be the solution of TSLasso problem*

$$J_{\lambda_n}(\mathbf{B}) = \frac{1}{2} \sum_{i=1}^n \|\mathbf{I}_d - \hat{\mathbf{X}}_i \mathbf{B}_i\|_F^2 + \frac{\lambda_n}{\sqrt{nd}} \|\mathbf{B}\|_{1,2}, \quad (39)$$

If $(1 + \tilde{\nu}_S/\delta^2)^2 \tilde{\mu}_S \tilde{\phi}_S \Gamma d < 1$ and $\lambda_n(1 + \tilde{\nu}_S/\delta^2)^2 < \tilde{b}_S \sqrt{n}/2$, there exists a positive constant c_0 such that if $e < c_0$ then $S(\hat{\mathbf{B}}) = S$.

Proof. The proof is direct by identifying the new $\tilde{\mu}'_S, \tilde{\nu}'_S$ parameters under noisy estimation of tangent space. The other parameters $\tilde{\phi}_S, \Gamma, \delta$ are not related with tangent spaces and thus remains unchanged.

Denote \hat{x}_{ij} the j -th column of $\hat{\mathbf{X}}_i$. Similarly, to (27a), we first bound

$$\begin{aligned}
\hat{x}_{ij}^\top \hat{x}_{ij'} &= \nabla f_j(\xi_i)^\top [\hat{\mathbf{T}}_i \hat{\mathbf{T}}_i^\top - \mathbf{T}_i \mathbf{T}_i^\top] \nabla f_{j'}(\xi_i) + \nabla f_j(\xi_i)^\top \mathbf{T}_i \mathbf{T}_i^\top \nabla f_{j'}(\xi_i) \\
&\leq \|\hat{\mathbf{T}}_i \hat{\mathbf{T}}_i^\top - \mathbf{T}_i \mathbf{T}_i^\top\|_2 \|\nabla f_j(\xi_i)\| \|\nabla f_{j'}(\xi_i)\| + \tilde{\mu}_S \|\nabla f_j(\xi_i)\| \|\nabla f_{j'}(\xi_i)\|, \quad \text{for all } j \in S, j' \notin S, i \in [n]
\end{aligned}$$

So $\tilde{\mu}'_S \leq \tilde{\mu}_S + e$.

By definition, let

$$\tilde{\tilde{\mathbf{X}}}_{iS} = \left[\frac{\hat{\mathbf{T}}_i^\top \nabla f_j(\xi_i)}{\|\nabla f_j(\xi_i)\|} \right]_{j \in S} = \hat{\mathbf{X}}_{iS} \mathbf{G}(\xi_i)^{-1}$$

where $\mathbf{G}(\xi_i) = \text{diag}\{||\nabla f_j(\xi_i)||\}_{j \in S}$ and then we have

$$\tilde{\nu}'_S = ||(\tilde{\tilde{\mathbf{X}}}_{iS}^\top \tilde{\tilde{\mathbf{X}}}_{iS})^{-1} - \mathbf{G}(\xi_i)^{-2}|| \leq \tilde{\nu}_S + ||(\tilde{\tilde{\mathbf{X}}}_{iS}^\top \tilde{\tilde{\mathbf{X}}}_{iS})^{-1} - (\tilde{\mathbf{X}}_{iS}^\top \tilde{\mathbf{X}}_{iS})^{-1}||$$

It suffices to upper bound the second term. We can apply lemma A.3, the perturbation bound of inverse of positive definite matrices. It suffice to compute

$$||(\tilde{\mathbf{X}}_{iS}^\top \tilde{\mathbf{X}}_{iS})^{-1}|| \leq ||(\tilde{\mathbf{X}}_{iS}^\top \tilde{\mathbf{X}}_{iS})^{-1} - \mathbf{G}_S(\xi_i)^2 + \mathbf{G}_S(\xi_i)^2|| \leq \tilde{\phi}_S^2 + \tilde{\nu}_S$$

And since for any $j, j' \in S$, it holds that

$$\begin{aligned} |(\tilde{\tilde{\mathbf{X}}}_{iS}^\top \tilde{\tilde{\mathbf{X}}}_{iS})_{jj'} - (\tilde{\mathbf{X}}_{iS}^\top \tilde{\mathbf{X}}_{iS})_{jj'}| &\leq ||\mathbf{T}_i \mathbf{T}_i^\top - \hat{\mathbf{T}}_i \hat{\mathbf{T}}_i^\top|| \leq e \\ ||\tilde{\tilde{\mathbf{X}}}_{iS}^\top \tilde{\tilde{\mathbf{X}}}_{iS} - \tilde{\mathbf{X}}_{iS}^\top \tilde{\mathbf{X}}_{iS}|| &\leq ||\tilde{\tilde{\mathbf{X}}}_{iS}^\top \tilde{\tilde{\mathbf{X}}}_{iS} - \tilde{\mathbf{X}}_{iS}^\top \tilde{\mathbf{X}}_{iS}||_F \leq de \end{aligned}$$

And thus we have

$$||(\tilde{\tilde{\mathbf{X}}}_{iS}^\top \tilde{\tilde{\mathbf{X}}}_{iS})^{-1} - (\tilde{\mathbf{X}}_{iS}^\top \tilde{\mathbf{X}}_{iS})^{-1}|| \leq (\tilde{\phi}_S^2 + \tilde{\nu}_S)^2 de$$

Hence $\tilde{\nu}'_S \leq \tilde{\nu}_S + (\tilde{\phi}_S^2 + \tilde{\nu}_S)^2 de$

For sufficiently small e , we will have $(1 + \frac{\tilde{\nu}'_S}{\tilde{\phi}_S^2})^2 \tilde{\mu}'_S \tilde{\phi}_S \Gamma d < 1$ and $\lambda_n(1 + \frac{\tilde{\nu}'_S}{\tilde{\phi}_S^2})^2 / \sqrt{n} < \frac{1}{2} \tilde{b}_S$ as these two inequality holds when $e = 0$. Then lemma A.6 guarantees exact recovery. \square

Proof of Proposition 4.2. With probability one, the following comparisons between sample based quantities and whole manifold versions holds:

$$\tilde{\mu}_S \leq \mu_S, \quad \tilde{\nu}_S \leq \nu_S, \quad \tilde{\phi}_S \leq \phi_S, \quad \tilde{b}_S \geq b_S \quad (40)$$

Let c_1, c_2 be the same as \tilde{c}_1, \tilde{c}_2 defined in the proof of theorem A.7, replacing all sample version quantities $\mu_S, \nu_S, \phi_S, b_S$ with their global manifold counterparts $\mu_S, \nu_S, \phi_S, b_S$.

Then the assumptions of the proposition guarantees that there exists a c_0 such that whenever $e < c_0$, exact recovery holds. It suffices to notice that

$$P(S(\hat{\mathbf{B}}) = S) \leq P(e < c_0) \geq 1 - 4 \left(\frac{1}{n} \right)^{\frac{2}{d}} \quad (41)$$

given by lemma A.8. \square

Lemma A.8 (Proposition in Aamari and Levrard [1]). *For sufficiently large C , let $r_N = C(\log n / (n - 1))^{1/d}$, tangent spaces $\hat{\mathbf{T}}_i$ estimated by WL-PCA in section 3.2 with linear kernel satisfy that with probability at least $1 - 4(1/n)^{2/d}$*

$$\max_{i=1:n} ||\mathbf{T}_i \mathbf{T}_i^\top - \hat{\mathbf{T}}_i \hat{\mathbf{T}}_i^\top|| = O(r_N) = O\left(\left(\frac{\log n}{n-1}\right)^{\frac{1}{d}}\right). \quad (42)$$

Remark A.9. Note that in this lemma, the hidden constant in big- O notation is determined by the manifold and sampling density.

B Additional Experimental Results

We include some additional experimental results and information in this section. The settings of two experiments on synthetic data are shown in table 2.

B.1 Results on Swiss Roll Data

We begin our experimental study by demonstrating that TSLASSO is invariant to the choice of embedding algorithm on the classic unpunctured SwissRoll dataset. This dataset consists of points sampled from a two dimensional rectangle and rolled up along one of the two axes aFigure 3a shows the SwissRoll dataset in \mathbb{R}^3 , then randomly rotated in $D = 49$ dimensions.

The dictionary \mathcal{F} consists of $g_{1,2}$, the two intrinsic coordinates, as well as $g_{j+2} = \xi_j$, for $j = 1, \dots, 49$, the coordinates of the feature space. Applying ManifoldLasso to the embeddings identifies the set $S = \{g_1, g_2\}$ as the manifold parametrization. This successful recovery of parametrizing functions is observed in each replicate. Figure 3b shows the regularization path in one replicates.

Dataset	n	N_a	D	d	ϵ_N	n'	p	ω
Swiss Roll	10000	NA	49	2	.18	100	51	1
Rigid Ethanol	10000	9	50	2	3.5	100	12	25

Table 2: Parameters in different experiments.

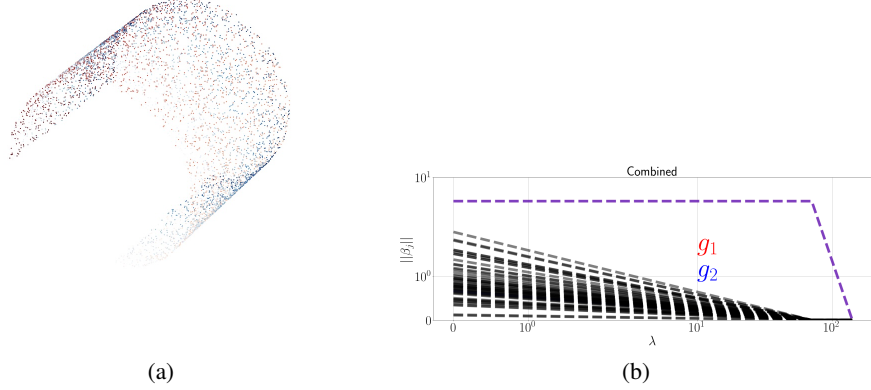


Figure 3: Swiss Roll data and result. **Left:** Unrotated swiss roll dataset in \mathbb{R}^3 . This dataset is then randomly rotated into \mathbb{R}^{49} . **Right:** The regularization path of TSLASSO on SwissRoll dataset in one replicate. Note that in fact there are two functions selected and their regularization path added together.

B.2 Results on Rigid Ethanol Dataset

We construct an ethanol skeleton composed of the atoms shown in Figure 2a. We then sample configurations as we rotate the atoms around the C-C and C-O bonds. In contrast with the MD trajectories, which are simulated according to quantum dynamics, these two angles are distributed uniformly over a grid, and Gaussian noise ($N_D(0, \sigma^2 I_D)$) is added to the position of each atom. We call the resultant dataset RigidEthanol. As expected given our two a priori known degrees of freedom, Figures 4a, 4b and 4c show that the estimated manifold is a two-dimensional surface with a torus topology similar to that observed for the MD Ethanol in Figure 8a. In particular, it is parameterized by bond torsions g_1 and g_2 . The dictionary contains the 12 torsions implicitly defined by the bond diagram, the same as the MDS real data experiment. The function pattern is also the same as the real ethanol dataset.

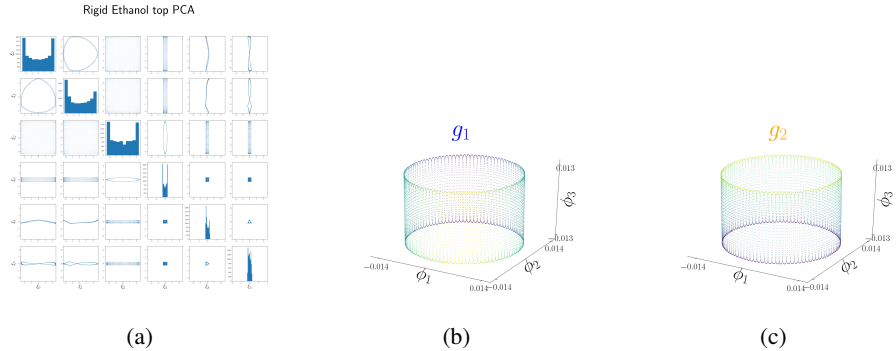


Figure 4: PCA features and Diffusion Map embedding features of rigid ethanol data without noise.

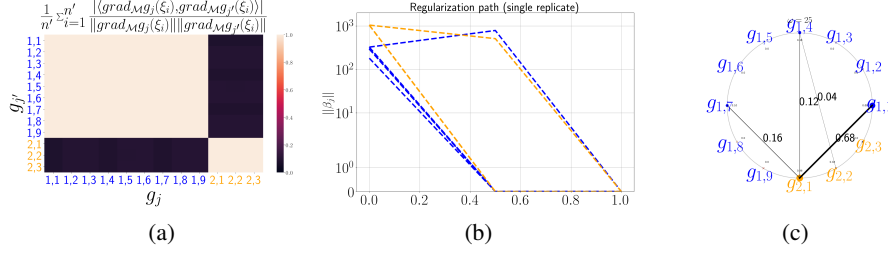


Figure 5: Results of Rigid Ethanol Experiment with no noise. **Left:** cosine plots of dictionary functions, showing the existence of two groups of highly colinear functions. **Middle:** regularization path in one replicate. **Right:** The frequency of each pair of function selected in all 25 replicates.

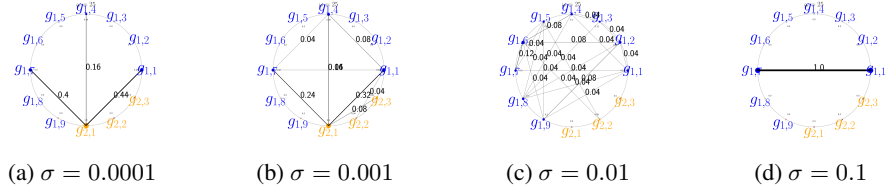


Figure 6: Watch plot of support recovery frequencies under different noise levels.

Figure 5a-5c show the result of experiments on rigid ethanol without any noise. We can tell from the result that over all 25 replicates, TSLASSO successfully recover the true support, one function from each colinear group.

With the increase in noise, we display the watch plot in figure 6a-6d. With the increase in the noise, it is possible that TSLASSO do not recover the correct support. For example when noise level is $\sigma = 0.1$, in all replicates, TSLASSO selects two functions in the same group. Interestingly, when we look at the embedding given by Diffusion Maps at this noise level, we observe that the torus topology is broken, as shown in figure 7a and 7b.

B.3 Comparison with Embeddings

The comparisons with Diffusion maps of Toluene are shown in the introduction in section 1. Here we display some comparison of TSLASSO with Diffusion maps on real MDS data, which are widely used for dimension reduction. Figure 8a and 8b shows that the two functions selected from the

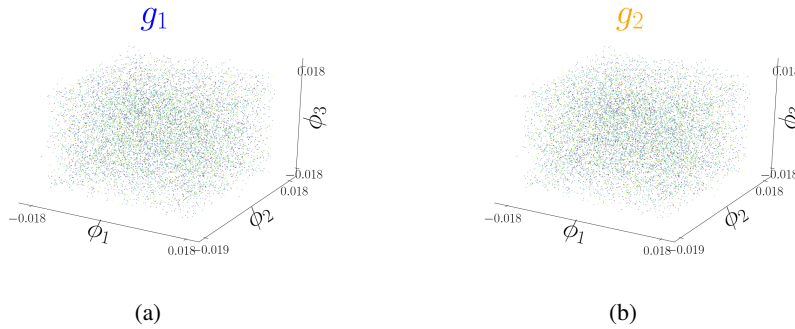


Figure 7: Diffusion map embedding for synthetic rigid ethanol data. Data points are colored by the true torsion g_1 and g_2 respectively.

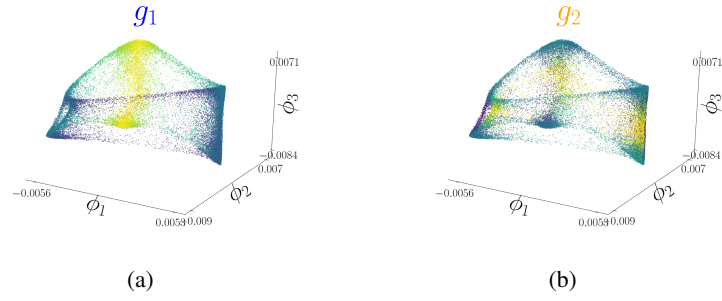


Figure 8: Diffusion map embedding for real ethanol data. Data points are colored by the two torsion functions g_0, g_9 found by TSLASSO respectively.

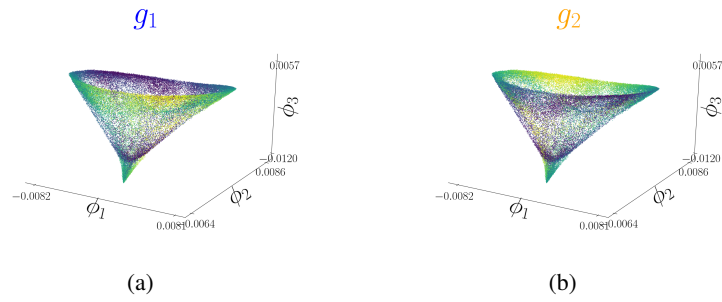


Figure 9: Diffusion map embedding for Malonaldehyde data. Data points are colored by the two torsion functions found by TSLASSO respectively.

TSLASSO indeed parametrizes the structure of the data. As the values are roughly varying along with two circles of the torus. Figure 9a and 9b shows a pair of functions selected by TSLASSO.